AD-A131 912 INTERACTION OF A DISLOCATION WITH A CRACK(U) PRINCETON UNIV NJ DEPT OF CIVIL ENGINEERING A C ERINGEN AUG 83 RR-83-SM-9 N00014-76-C-0240 1/1

UNCLASSIFIED F/G 12/1 NL

END
DATE
FILMED
9-83
DTIC

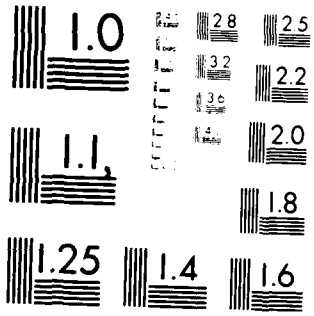

MICROCOPY RESOLUTION TEST CHART
NATIONAL BUREAU OF STANDARDS 1963-A

AD A 131912

INTERACTION OF A DISLOCATION WITH A CRACK

A. Cemal Eringen
PRINCETON UNIVERSITY

Technical Report No. 59
Civil Engng. Res. Rep. No. 83-SM-9

AUG 3 0 1983
A

Research Sponsored by the
OFFICE OF NAVAL RESEARCH
under
Contract N00014-76-C-0240 Mod 4
Task No. NR 064-410

Aug. 1983

Approved for public release:
distribution unlimited

Reproduction in whole or in part is permitted
for any purpose of the United States Government

DTIC FILE COPY

83 08 26 064

INTERACTION OF A DISLOCATION WITH A CRACK

A. Cemal Eringen
Princeton University
Princeton, NJ 08544

ABSTRACT

A solution is given of the field equations of nonlocal elasticity for a line crack interacting with a screw dislocation in an elastic plane under anti-plane shear loading. Displacement and stress fields are determined throughout the core region and beyond. In the case when the dislocation is absent, the circumferential stress is shown to vanish at the crack tip, increasing to a maximum along the crack line afterwards decreasing to its classical value at large distances from the crack tip. This is in contradiction with the classical elasticity solutions which predicts stress singularity at the crack tip and it is in accordance with the physical condition that the crack tip surface must be free of surface tractions. The presence of the dislocation alters the stress distribution considerably when it is close to the crack tip. The stress distributions, in the core region, are displayed. A fracture criterion based on the maximum stress is established and used to determine the theoretical strengths of pure crystals that contain a line crack. Results are in good agreement with those based on the atomic theories and experiments.

SECURITY CLASSIFICATION OF THIS PAGE (When Data Entered)

REPORT DOCUMENTATION PAGE		READ INSTRUCTIONS BEFORE COMPLETING FORM
1 REPORT NUMBER PRINCETON UNIV. TECHNICAL REPORT #59	2 GOVT ACCESSION NO.	3 RECIPIENT'S CATALOG NUMBER
4 TITLE (and Subtitle) INTERACTION OF A DISLOCATION WITH A CRACK		5 TYPE OF REPORT & PERIOD COVERED Technical Report
		6 PERFORMING ORG. REPORT NUMBER 83-SM-9
7 AUTHOR(s) A. Cemal Eringen		8 CONTRACT OR GRANT NUMBER(s) N00014-76-002040 Mod. 4
9 PERFORMING ORGANIZATION NAME AND ADDRESS PRINCETON UNIVERSITY Princeton, NJ 08544		10 PROGRAM ELEMENT, PROJECT, TASK AREA & WORK UNIT NUMBERS NR 064-410
11 CONTROLLING OFFICE NAME AND ADDRESS OFFICE OF NAVAL RESEARCH (Code 471) Arlington, VA 22217		12 REPORT DATE Aug. 1983
		13 NUMBER OF PAGES 30
14 MONITORING AGENCY NAME & ADDRESS(if different from Controlling Office)		15 SECURITY CLASS (of this report) unclassified
		15a DECLASSIFICATION DOWNGRADING SCHEDULE

16 DISTRIBUTION STATEMENT (of this Report)

17 DISTRIBUTION STATEMENT (of the abstract entered in Block 20, if different from Report)

18 SUPPLEMENTARY NOTES

19 KEY WORDS (Continue on reverse side if necessary and identify by block number)

dislocation, crack, fracture, interaction of dislocation and crack, nonlocal elasticity

20 ABSTRACT (Continue on reverse side if necessary and identify by block number)

A solution is given of the field equations of nonlocal elasticity for a line crack interacting with a screw dislocation in an elastic plane under anti-plane shear loading. Displacement and stress fields are determined throughout the core region and beyond. In the case when the dislocation is absent, the circumferential stress is shown to vanish at the crack tip, increasing to a maximum along the crack line afterwards decreasing

DD FORM 1 JAN 73 1473 EDITION OF 1 NOV 65 IS OBSOLETE (cont)

SECURITY CLASSIFICATION OF THIS PAGE (When Data Entered)

ABSTRACT (cont)

to its classical value at large distances from the crack tip. This is in contradiction with the classical elasticity solutions which predicts stress singularity at the crack tip and it is in accordance with the physical condition that the crack tip surface must be free of surface tractions. The presence of the dislocation alters the stress distribution considerably when it is close to the crack tip. The stress distributions, in the core region, are displayed. A fracture criterion based on the maximum stress is established and used to determine the theoretical strengths of pure crystals that contain a line crack. Results are in good agreement with those based on the atomic theories and experiments.

I. INTRODUCTION

It is well known that the classical elasticity solution of crack problems fail in a core region around a sharp crack tip, since they predict stress singularity at the tip. The assessment of the core radius and the stress field within the core is a problem usually discussed within the context of atomic theories of lattices (cf. [1]), even at that its treatment contains various assumptions regarding the interatomic arrangements and force fields.

Engineering fracture mechanics, on the other hand, is based on the Griffith's[2] ideas which resort to other concepts (e.g. energy, J-integral, fracture toughness). To be sure, there exist certain erzatz to account for the effect of the core region on fracture process in phenomenological ways. These are useful for engineering purposes, however, they are not based on a fundamental theory nor are they capable predicting the state of stress in the core region whcih is fundamental to the initiation of fracture.

In several previous papers, we have shown that nonlocal elasticity solutions of Griffith crack problems lead to finite stress at the crack tip[3-5]. In fact, an exact solution[6] obtained for the screw dislocation, indicates that the stress vanishes at the tip of the crack, growing to a maximum in the vicinity of the crack tip. The important implications of this result in connection with the initiation of fracture is the motivation for the present work.

The solution obtained here for the Mode III (anti-plane shear) problem for a crack interacting with a screw dislocation indicates that the circumferential stress field is vanishingly small (zero when the dislocation

is absent) at the crack tip, when the screw is located far away from the crack tip. When the dislcoation is near the crack tip, the stress field is affected apprciably displaying several maxima near the crack tip. By equating the maximum stress to the cohesive yield stress, we can determine the stress intensity factor K_g or the theoretical yield stress, given K_g. Calculated K_g values, on the basis of the present theory, are in fair agreement with those determined experimentally. Theoretical strengths are also estimated by means of the dislocation model. Results agree with those predicted by atomic models.

The mathematical model of approach to the solution of this problem is new and possesses potential applications in other areas.

2. BASIC EQUATIONS

In several previous papers, we developed a theory of nonlocal elasticity, cf. [7, 8, 9]. For homogeneous and isotropic elastic solids, linear theory is expressed by the set of equations

$$t_{k\ell,k} + \rho(f_\ell - \ddot{u}_\ell) = 0 , \tag{2.1}$$

$$t_{k\ell}(\underset{\sim}{x},t) = \int_V \alpha(|\underset{\sim}{x}'-\underset{\sim}{x}|, \tau)\, \sigma_{k\ell}(\underset{\sim}{x}',t)\, dv(\underset{\sim}{x}') , \tag{2.2}$$

$$\sigma_{k\ell}(\underset{\sim}{x}',t) = \lambda\, e_{rr}(\underset{\sim}{x}',t)\, \delta_{k\ell} + 2\,\mu\, e_{k\ell}(\underset{\sim}{x}',t) , \tag{2.3}$$

$$e_{k\ell}(\underset{\sim}{x}',t) = \frac{1}{2}\left[\frac{\partial u_k(\underset{\sim}{x}',t)}{\partial x'_\ell} + \frac{\partial u_\ell(\underset{\sim}{x}',t)}{\partial x'_k}\right] \tag{2.4}$$

where $t_{k\ell}$, ρ, f_ℓ and u_ℓ are respectively, the stress tensor, mass density, body force density and the displacement vector. λ and μ are the Lamé elastic constants and α is the "attenuation function" which depends on the distance $|\underset{\sim}{x}'-\underset{\sim}{x}|$ and a parameter τ which denotes the ratio of the internal characteristic length a to the external characteristic length ℓ, i.e.

$$\tau = e_0 \, a/\ell \tag{2.5}$$

where e_0 is a constant appropriate to each material. Characteristic lengths may be selected according to the range and sensitivity of the physical phenomena to be investigated. For instance, for perfect crystals, a may be taken as the lattice parameter and ℓ as the half crack length. For granular materials, a may be considered to be the average granular distance and for fiber composites, the fiber distance etc. The <u>material constant</u>, e_0 may be determined by one experiment.

Equations (2.1), (2.3) and (2.4) are those known from the theory of classical elasticity, but Eq. (2.2) is new, replacing Hooke's law. According to Eq. (2.2), the stress at a point $\underset{\sim}{x}$ depends on strains at <u>all points</u> $\underset{\sim}{x}'$ of the body. The attenuation function α determines the degree of influence with the distance. From the physical nature of solids, it is clear that the influence of strains at $\underset{\sim}{x}'$, on the stress at $\underset{\sim}{x}$, decreases with the distance $|\underset{\sim}{x}'-\underset{\sim}{x}|$. Thus, $\alpha(|\underset{\sim}{x}'-\underset{\sim}{x}|)$ must acquire its maximum at $\underset{\sim}{x}'=\underset{\sim}{x}$. Moreover, when $a \to 0$, α must become a Dirac delta measure so that nonlocal theory shall revert to classical elasticity theory. By matching the phonon dispersion curves with those resulting from nonlocal theory, we have determined α for various cases (cf. [5], [8], [10]).

By discretizing Eq. (2.2), it can be shown that equations of nonlocal elasticity revert to those of atomic lattice dynamics.[11] Thus, it is clear that nonlocal theory is a suitable model for the treatment of physical phenomena with characteristic lengths in the range from the molecular or atomic dimensions to macroscopic sizes.

For a two-dimensional perfect lattice, the dispersion curves are matched in the entire Brillouin zone to within an error less than $1\frac{1}{2}\%$ with the attenuation function[10]

$$\alpha(|\underset{\sim}{x}|, \tau) = (2\pi\ell^2\tau^2)^{-1} K_0(\sqrt{\underset{\sim}{x}\cdot\underset{\sim}{x}}/\ell\tau) \tag{2.6}$$

where K_0 is the modified Bessel's function. We note that Eq. (2.6) is Green's function for the operator $L \equiv (1 - \ell^2\tau^2\nabla^2)$, i.e.

$$(1 - \ell^2\tau^2\nabla^2)\alpha = \delta(|\underset{\sim}{x}'-\underset{\sim}{x}|) \tag{2.7}$$

In fact, it is possible to employ other linear operators to characterize the nature of nonlocal attractions of material points in solids. This apparent non-uniqueness of α may be considered to be a defect of the theory. On the contrary, for imperfect and amorphous solids, this may provide a desirable flexibility. Ultimately, however, α should be determined from experimental and/or statistical mechanical considerations. For perfect crystals, Eq. (2.6) leads to excellent agreements with the dispersion curves based on atomic lattice theory.

Upon the application of the operator, $L \equiv 1 - \ell^2\tau^2\nabla^2)$ to Eq. (2.2), we obtain

$$(2.8) \qquad (1 - \ell^2\tau^2\nabla^2)\, t_{k\ell} = \sigma_{k\ell}$$

Divergence of Eq. (2.8), upon using (2.1) and (2.3), leads to

$$(2.9) \qquad (\lambda+\mu)\, u_{k,k\ell} + \mu\, u_{\ell,kk} + (1 - \ell^2\tau^2\nabla^2)(\rho f_\ell - \rho \ddot{u}_\ell) = 0$$

For the static case and vanishing body forces, Eq. (2.9) is non other than Navier's equation of classical elasticity. Note, however, that the stress tensor is not $\sigma_{k\ell}$ but $t_{k\ell}$ and it requires that we solve Eq. (2.8) to determine $t_{k\ell}$.

For plane, harmonic, SH-waves, Eq. (2.9) gives the frequency

$$(2.10) \qquad \omega = (\mu/\rho)^{\frac{1}{2}}\, k[1 + e_0^2 k^2 a^2]^{-\frac{1}{2}}$$

where k is the amplitude of the wave vector. By equating ω given by Eq. (2.10) to that predicted by the Born-Kármán model of lattice dynamics, at the end of the Brillouin zone $(ka = \pi)$, we find that

$$(2.11) \qquad e_0 = (\pi^2 - 4)^{\frac{1}{2}}/2\pi = 0.39\,.$$

The dispersion curve based on Eq. (2.10) and that of the Born-Kármán model are compared in Fig. 1. We see that the matching is very good. The maximum error is less than 6%.

The dispersion curves of the Born-Kármán model is a good approximation for some fcc and bcc metals (e.g. Al and cu). While the Brillouin zone may vary in different directions of slips in crystals, we believe that Eq. (2.11) is a reasonable value for e_0 when the material is considered to be isotropic.

3. CLASSICAL STRESS FIELDS

A homogeneous, isotropic elastic solid of infinite extent contains a crack located at $-c \leq x_1 \leq c$, $x_2 = 0$, $-\infty < x_3 < \infty$ where x_k are the rectangular coordinates, Fig. 2. We suppose that there exists a dislocation which lies parallel to the x_3-axis and which intersects the plane $x_3 = 0$ at the point $S\{x_1 = \xi, \ x_2 = \eta\}$. The solid is subject to a constant anti-plane shear at $x_2 = \pm\infty$. The classical elasticity solution of this problem was given by Louat[12]. However, here we derive the solution of this problem in the form better suited for our purpose, eliminating possible misprints, difficulties in notations and in taking various limits.

Since the state of the body is the same at all planes, $x_3 = \text{const.}$, the problem is two-dimensional and we need to treat the plane problem in the plane $x_3 = 0$ with a line crack located at $x_2 = 0$, $|x_1| \leq c$.

The classical stress field at any point $P(x_1, x_2)$ may be expressed conveniently in the form

$$\sigma_{23} - i\,\sigma_{13} = A\int_{-c}^{c} \frac{f(t)}{\bar{z}-t}\,dt \qquad , \tag{3.1}$$

where $\bar{z} = x_1 - i\,x_2$ and $f(t)$ is the distribution function which is the solution of the equation of equilibrium of the forces acting on the crack surface:

$$A\int_{-c}^{*c} \frac{f(t)}{t-x}\,dt = \sigma_d(x) + \sigma_0\,, \qquad A = \mu\lambda_0/2\pi \tag{3.2}$$

Here, the integral denotes a Cauchy principal value, μ is the shear modul λ_0 is the displacement vector of a unit positive dislocation and σ_0 and σ_c are the stress fields at the crack surface due to the applied load and the dislocation, respectively.

The solution of the integral equation (3.2) is well-known, Tricomi[13]

$$f(x) = -\frac{1}{\pi^2 A\sqrt{c^2-x^2}}\int_{-c}^{*c} \sqrt{c^2-t^2}\;[\sigma_0 + \sigma_d(t)]\,\frac{dt}{t-x} + \frac{Q}{\sqrt{c^2-x^2}} \tag{3.3}$$

Here, Q is a constant to be determined from the condition that

$$\int_{-c}^{c} f(x)\,dx = n \tag{3.4}$$

where $n\lambda_0$ is the total dislocation content of the distribution $f(x)$.

The stress $\sigma_d(t)$ is given by

$$\sigma_d(t) = \frac{\mu b(t-\xi)}{2\pi[(t-\xi)^2 + \eta^2]} \tag{3.5}$$

Substituting this into Eq. (3.3), we can carry out integrations to obtain

$$f(x) = \frac{1}{\sqrt{c^2-x^2}} \left\{ \frac{\sigma_0 x}{\pi A} - \frac{b}{\pi\lambda_0} \left[\frac{\sqrt{\zeta^2-c^2}}{2(\zeta-x)} + \frac{\sqrt{\bar{\zeta}^2-c^2}}{2(\bar{\zeta}-x)} - 1 \right] + Q \right\} \tag{3.6}$$

where $\zeta = \xi + i\eta$, $\bar{\zeta} = \xi - i\eta$. Using this in Eq. (3.4), we will have $Q = n/\pi$. Carrying $f(x)$ into Eq. (3.1) after some tedious integrations, we obtain

$$\sigma_{23} - i\,\sigma_{13} = \sigma_0\left(\frac{\bar{z}}{\sqrt{\bar{z}^2-c^2}} - 1\right) - \frac{bA}{2\lambda_0}\left[\frac{1}{\bar{z}-\zeta}\left(1 - \frac{\sqrt{\zeta^2-c^2}}{\sqrt{\bar{z}^2-c^2}}\right) + \frac{1}{\bar{z}-\bar{\zeta}}\left(1 - \frac{\sqrt{\bar{\zeta}^2-c^2}}{\sqrt{\bar{z}^2-c^2}}\right)\right] + \left(\frac{b}{\lambda_0} + n\right)\frac{A}{\sqrt{\bar{z}^2-c^2}} \tag{3.7}$$

The forces acting on the dislocation at (ξ,η), due to the crack, are given by

$$F_1 = b\,\sigma_{23}, \qquad F_2 = b\,\sigma_{13} \qquad (x_1 = \xi\ ,\ \ x_2 = \eta) \tag{3.8}$$

For our own purpose later, we need the stress field when the dislocation is located along the x_1-axis and the surface of the crack is free of tractions. To this end, we set $\eta = 0$ and add

(3.9) $$\sigma_0 + \sigma_d(x_1) = \sigma_0 + \frac{bA}{\lambda_0(\bar{z} - \xi)}$$

to the right-hand side of Eq. (3.7). Hence,

(3.10) $$\sigma_{23} - i\,\sigma_{13} + \sigma_0 + \sigma_d(x_1) = \frac{1}{\sqrt{\bar{z}^2 - c^2}}\left[\sigma_0\,\bar{z} + A\left(\frac{b}{\lambda_0} + n\right) + \frac{bA}{\lambda_0}\,\frac{\sqrt{\xi^2 - c^2}}{\bar{z} - \xi}\right]$$

gives the classical stress field at any point outside of the crack when the body is loaded at $x_2 = \pm\infty$ with a constant shear $\sigma_{23} = \pm\sigma_0$. When the crack contains no dislocations, then we have $n = 0$.

Two special cases are important:

(i) *No Crack and* $\sigma_0 = 0$. In this case, the classical stress field is given by

(3.11) $$\sigma = \frac{\mu b}{2\pi\,\bar{z}}$$

where we also set $\xi = 0$ placing the dislocation to the origin of coordinates.

(ii) *No Dislocations*. In this case, $A = 0$ and we have

(3.12) $$\sigma = \frac{\sigma_0\bar{z}}{\sqrt{\bar{z}^2 - c^2}}$$

Both of these results are well-known in the literature.

4. NONLOCAL STRESS FIELDS

To determine the nonlocal stress fields, we must obtain the solution of

$$(1 - \tau^2 \ell^2 \nabla^2)\, t = \sigma \tag{4.1}$$

subject to some boundary conditions. Here

$$t = t_{23} - i\, t_{13}, \qquad \sigma = \sigma_{23} - i\, \sigma_{13} + \sigma_0 + \sigma_d(x_1) \tag{4.2}$$

Since $\nabla^2 \sigma = 0$, $t = \sigma$ is a particular solution of Eq. (4.1). The complementary solution of (4.1), vanishing at infinity and having proper symmetry regulations with respect to $(x_1, \pm x_2)$, is of the form

$$t_c = K_\nu(r/\ell\tau)(A_\nu\, e^{i\nu\theta} + B_\nu\, e^{-i\nu\theta}) \tag{4.3}$$

where A_ν, B_ν and ν are constants, $K_\nu(\rho)$ is the modified Bessel's function and (r,θ) are the plane polar coordinates.

The boundary condition on the crack surface requires that $t_{23} = 0$. Taking the origin $r = 0$ of the coordinates at the right-hand crack tip and writing $r = r_1$, $\theta = \theta_1$, in (4.3) we see that to fulfill this condition, we must have $\nu = 1/2$, since all other solutions lead to displacement singularities at $r_1 = 0$.

Classical stress field σ possesses singularity at the screw dislocation $x_1 = \xi$, $x_2 = 0$. The surface traction, t_{rz} on the edge surface of the dislocation is required to vanish, according to the boundary

condition. To fulfill this condition we take $\nu = 1$ and move the origin of coordinates to $x_1 = \xi$, $x_2 = 0$. This may be expressed by writing $r = r_d$, $\theta = \theta_3$ and

$$r_d e^{i\theta_3} = r_1 e^{i\theta_1} - x_0 . \tag{4.4}$$

Hence, the general solution of (4.1) appropriate to our problem is of the form

$$\begin{aligned} t = {} & (\pi\tau\ell/2r_1)^{\frac{1}{2}} e^{-r_1/\tau\ell} (C_1 e^{i\theta_1/2} + C_2 e^{-i\theta_1/2}) \\ & + K_1(r_d/\tau\ell)(C_3 e^{i\theta_3} + C_4 e^{-i\theta_3}) + \sigma . \end{aligned} \tag{4.5}$$

To determine C_α, we calculate stress components in polar coordinates (r_1, θ_1):

$$t_{\theta z} - i\, t_{rz} = (t_{23} - i\, t_{13})\, e^{-i\theta_1} . \tag{4.6}$$

We imagine the crack tip as a limit of a small circular arc with radius $r_1 = \varepsilon$ approaching zero. For small ε, we have approximately

$$\begin{aligned} z &= c + z_1 = -c + z_2 = \xi + z_3 = c + x_0 + z_3 , \\ z_1 &= \varepsilon e^{i\theta_1} . \end{aligned} \tag{4.7}$$

Using these in Eq. (3.10), we will have

$$(4.8) \qquad \sigma = (c/2r_1)^{\frac{1}{2}} e^{i\theta_1/2} \left[\sigma_0 + \frac{\mu b}{2\pi c}\left(1+\frac{n\lambda_0}{b_0}\right) - \frac{\mu b}{2\pi c}\left(1 + \frac{2c}{x_0}\right)^{\frac{1}{2}}\right]$$

Consequently, Eq. (4.5) gives

$$(4.9) \qquad t_{\theta z} - i\, t_{rz} = (c/2r_1)^{\frac{1}{2}} e^{-i\theta_1/2}\left[\sigma_0 + \frac{\mu b}{2\pi c}\left(1+\frac{n\lambda_0}{b}\right) - \frac{\mu b}{2\pi c}\left(1 + \frac{2c}{x_0}\right)^{\frac{1}{2}}\right]$$
$$+ (\pi\tau\ell/2r_1)^{\frac{1}{2}} e^{-r_1/\tau\ell}\left(C_1 e^{-i\theta_1/2} + C_2 e^{-3i\theta_1/2}\right)$$
$$+ K_1(|x_0|/\tau\ell)\left(C_3 \frac{r_1}{x_0} e^{i\theta_1} - C_3 + C_4 \frac{r_1}{x_0} e^{-i\theta_1} - C_4\right) e^{-i\theta_1}$$

The boundary condition on t_{rz} requires that

$$(4.10) \qquad \lim_{r_1 \to 0} t_{rz} = 0$$

This condition will be fulfilled approximately* for $x_0/\tau\ell \gg 1$ if $C_2 = 0$ and

$$(4.11) \qquad C_1 = -(c/\pi\tau\ell)^{\frac{1}{2}}\left[\sigma_0 + \frac{\mu b}{2\pi c}\left(1 + \frac{n\lambda_0}{b}\right) - \frac{\mu b}{2\pi c}\left(1 + \frac{2c}{x_0}\right)^{\frac{1}{2}}\right]$$

Next, we calculate the stress field at the location $r_d = 0$ of the screw dislocation. As $r_d \to 0$ we have $r_1 = x_0$ and

---

*In fact, this condition is satisfied exactly along the crack line $\theta_1 = \pm\pi$.

$$(4.12)\quad t_{z\theta} - i\, t_{zr} = (\pi\tau\ell/2x_0)^{\frac{1}{2}}\, e^{-x_0/\tau\ell} C_1 + K_1(r_d/\tau\ell)(C_3\, e^{i\theta_3} + C_4\, e^{-i\theta_3})$$

$$+ [x_0(x_0+2c)]^{-\frac{1}{2}}[\sigma_0(c+x_0) + \frac{\mu b}{2\pi}(1+\frac{n\lambda_0}{b})$$

$$+ \frac{\mu b}{2\pi r_d}[x_0(x_0+2c]^{\frac{1}{2}}\, e^{i\theta_3} \quad .$$

Again t_{zr} must vanish as $r_d \to 0$. This implies that $C_4 = 0$ and

$$(4.13)\qquad C_3 = -\mu b/2\pi\tau\ell \ .$$

The general solution is now complete.

$$(4.14)\quad t = (\pi\tau\ell/2r_1)^{\frac{1}{2}}\, e^{-r_1/\tau\ell}\, C_1\, e^{i\theta_1/2} + K_1(r_d/\tau\ell)\, C_3\, e^{i\theta_3} + \sigma$$

where C_1 and C_3 are given by (4.11) and (4.13). In polar coordinates, we have

$$(4.15)\quad t_{\theta z} - i\, t_{rz} = (\pi\tau\ell/2r_1)^{\frac{1}{2}}\, e^{-r_1/\tau\ell} C_1\, e^{-i\theta_1/2} + K_1(r_d/\tau\ell)\, C_3\, e^{i(\theta_3-\theta_1)}$$

$$+ (r_1 r_2)^{-\frac{1}{2}}\, e^{i(\theta_2-\theta_1)/2}\Big\{[\sigma_0\, r\, e^{-i\theta} + \frac{\mu b}{2\pi}(1 + \frac{n\lambda_0}{b})$$

$$+ \frac{\mu b}{2\pi}(r_1\, e^{-i\theta_1} - x_0)^{-1}\, [x_0(x_0+2c)]^{\frac{1}{2}}\Big\}$$

Special cases mentioned in Section 3 can be obtained in a similar fashion.

(i) *No Crack*

$$t_{\theta z} - i\, t_{rz} = \frac{\mu b}{2\pi\tau\ell}\,\frac{1}{\rho}\,[1 - \rho\, K_1(\rho)]\ , \tag{4.16}$$

where we have taken the origin of the polar coordinates at the dislocation, so that $\rho = r_d/\tau\ell$.

(ii) *No Dislocation*

$$t_{\theta z} - i\, t_{rz} = \sigma_0 (c/2r_1)^{\frac{1}{2}}\, [(2r^2/cr_2)^{\frac{1}{2}}\, e^{i(-\theta + \frac{2}{2})} - e^{-r_1/\tau\ell}]\, e^{-i\theta_1/2} \tag{4.17}$$

5. FRACTURE

Here, we discuss the onset of fracture and determine the theoretical stresses for the two special cases.

(i) No Crack

According to Eq. (4.16), we have $t_{rz} = 0$ and

$$T_\theta(\rho) = \frac{2\pi\tau\ell}{\mu b}\, t_{\theta z} = \rho^{-1}[1 - \rho K_1(\rho)] \tag{5.1}$$

The maximum of T_θ occurs at $\rho = 1.1$ and is given by

$$T_{\theta max} = 0.3993\ ; \qquad \rho_c = 1.1 \tag{5.2}$$

It is natural to assume that when $t_{\theta z\,max}$ becomes equal to the theoretical stress t_y, the crystal will rupture. Thus,

$$t_y/\mu \simeq 0.3993 \frac{b}{2\pi e_0 a} \tag{5.3}$$

If we write $h = e_0 a/0.3993$, this agrees with the estimate of Frenkel based on an atomic model (cf. Kelly[14], p. 12). For aluminum (fcc), $b = a/\sqrt{2}$ and for iron (bcc), $b = \sqrt{3}/2$, so that Eq. (5.3) gives

$$t_y/\mu = 0.12 \qquad \{\text{Al: } [111]\langle 1\bar{1}0\rangle\}$$

$$t_y/\mu = 0.14 \qquad \{\text{Fe: } [1\bar{1}0]\langle 111\rangle\}$$

These are close to the theoretical results $t_y/\mu = 0.11$ based on atomic models.

It is interesting to note that $t_{\theta z} = 0$ at the center of dislocation and it rises to a maximum at $\rho = 1.1$, thereafter decreasing to zero with ρ. Significant consequences of the present predictions as contrasted to the classical results are:

(a) The stress at the center of the core is <u>not</u> infinite, but zero.

(b) Fracture begins at $\rho = \rho_c$ not at the center of the core.

(c) There is a low stress region, $0 < \rho < \rho_c$ within the core.

(ii) *<u>No Dislocations</u>*

From (4.17), it is clear that $t_{\theta z}$ acquires its maximum along the crack line $\theta = \theta_1 = \theta_2 = 0$, near the crack tip. The circumferential stress along

the crack line $r_1 \geq 0$ is expressed by

$$(5.4) \qquad t_{z\theta}/\sigma_0 = (2\gamma\rho)^{-\frac{1}{2}} \left[(1 + \gamma\rho)(1 + \tfrac{\gamma\rho}{2})^{-\frac{1}{2}} - e^{-\rho}\right]$$

where

$$(5.5) \qquad \rho = r_1/e_0 a\,, \qquad\qquad \gamma = e_0 a/c$$

$t_{z\theta}$ vanishes at the crack tip $\rho = 0$ and has a maximum at $\rho = \rho_c$ which is the root of

$$(5.6) \qquad e^{-\rho}\,(1 + 2\rho) \;\approx\; (1 + \tfrac{\gamma\rho}{2})^{-3/2}$$

Since $\gamma \ll 1$ $(\gamma \leq 10^{-6})$, we see that the root of (5.6) is independent of c and is given by

$$(5.7) \qquad \rho_c \;\approx\; 1.2565$$

and the maximum stress is given by

$$(5.8) \qquad t_{z\theta\ \max} \;=\; \sigma_0 (e_0 a/c)^{-\frac{1}{2}} \left(\sqrt{2\rho_c} + \frac{1}{\sqrt{2\rho_c}}\right)^{-1} .$$

We also observe that as $\rho \to \infty$, (5.4) gives $t_{z\theta} = \sigma_0$, as it should.

In the classical tradition, if we write $K_{III} = \sqrt{\pi c}\,\sigma_0$, then (5.4) may be expressed as

$$(5.9) \qquad T_\theta(\rho) = \sqrt{\gamma}\, t_{z\theta}/\sigma_0 = (\pi\, e_0 a)^{\frac{1}{2}}\, t_{z\theta}/K_{III}$$

$$= (2\rho)^{-\frac{1}{2}} [1 + \gamma\rho)(1 + \frac{\gamma\rho}{2})^{-\frac{1}{2}} - e^{-\rho}]$$

This is plotted against ρ , in Fig. 3 in the vicinity of the crack tip. The classical (local) stress is also indicated on this figure by dashed lines. From this figure, it is clear that the classical stress field deviates considerably from the nonlocal stress field in the region $0 \leq \rho < 5$. In fact, it diverges at the crack tip.

A <u>perfect crystal</u> which contains a crack, but no dislocation, will not rupture before the maximum stress reaches the value of the cohesive stress (theoretical stress) that holds the atomic bonds of the lattice. Thus, the entire crystal is in the elastic state of equilibrium when

$$(5.10) \qquad t_{z\theta\,max} < t_y \,.$$

The failure begins when $t_{z\theta max} = t_y$, i.e., when

$$(5.11) \qquad K_c/t_y = (\pi\, e_0 a)^{\frac{1}{2}} (\sqrt{2\rho_c} + \frac{1}{\sqrt{2\rho_c}}) = 3.9278 \sqrt{e_0 a}$$

where $K_c = \sqrt{\pi c}\, \sigma_{0c}$ is the critical fracture toughness.

Using Eq. (5.11) and $e_0 = 0.39$, we calculate a few K_g-values which are listed in Table 1 (last column) along with classical K_c's based on $K_c = 4\mu\gamma_s)^{\frac{1}{2}}$, where γ_s is the surface energy. Experimental observations

of Ohr and Chang[15,16] are also listed in this Table. Classical estimates are expected to be inaccurate considering the fact that even with the best present-day techniques available, they could not be measured to an accuracy better than a factor of two. Moreover, classical formula assumes no defects (i.e., no crack and dislocation), therefore it is expected to give higher K_c-values. On the other hand, experimental measurements of Ohr and Chang required the measurement of the length of the plastic zone among other constants. This already implies the existence of dislocations so that we expect some deviation from the perfect crystal containing no dislocation but a single crack. In Section 6, we examine the general case when the solid contains a crack and a dislocation.

6. DISLOCATION AND CRACK

Along the crack line $x_1 \geq c, \; x_2 = 0$,

Eq. (4.15) gives $t_{rz} = 0$ and with $n = 0$

$$t_{\theta z} = t^c + t^{dc} \tag{6.1}$$

where

$$t^c \sqrt{\gamma} \,/\, \sigma_0 \equiv T_1 = (2\rho)^{-\frac{1}{2}} \left[1 + \gamma\rho)(1 + \frac{\gamma\rho}{2})^{-\frac{1}{2}} - e^{-\rho}\right], \tag{6.2}$$

$$t^{dc} \sqrt{\gamma} \,/\sigma_0\beta \equiv T_2 = (2\rho)^{-\frac{1}{2}} \Big\{ \left[(1+\frac{\gamma\rho}{2})^{-\frac{1}{2}} - [1 - (1+ \frac{2}{\gamma\bar{x}_0})^{\frac{1}{2}}]e^{-\rho}\right.$$
$$\left. - \operatorname{sgn}(\rho-\bar{x}_0)(2\rho/\gamma)^{\frac{1}{2}} K_1(|\rho-\bar{x}_0|) + (1+ \frac{\gamma\rho}{2})^{-\frac{1}{2}} (1+\frac{2}{\gamma\bar{x}_0})^{\frac{1}{2}}(\frac{\rho}{\bar{x}_0} -1)^{-1} \right\} \tag{6.3}$$

in which

$$(6.4) \qquad \bar{x}_0 = x_0/e_0 a \ , \quad \beta = \frac{\mu b}{2\pi c \sigma_0}$$

when the dislocation is absent we have $t^{dc} = 0$ so that t^{dc} is the shear stress arising from the interaction of the dislocation with the crack. At the crack tip $\rho = 0$ and we have

$$(6.5) \qquad t_{\theta z} / \sigma_0 \beta = \frac{1}{\gamma} K_1(\bar{x}_0)$$

This shows that for positive dislocation ($b>0$) the shear stress is positive and therefore the crack tip will tend to close up for $b>0$. For $b<0$ the opposite will occur. However, the stress given by (6.5) due to the dislocation is very small for large $\bar{x}_0$ and it becomes large when the dislocation is very close to the crack tip. The stress field $T_1(\rho) \equiv T_\theta(\rho)$ so that Fig. 3 represents $T_1(\rho)$. Fig. 4 displays graphs of $T_2(\rho)$ for several values of $\bar{x}_0 = 3.1, 4.1, 6.1$ and 10.1, keeping $\gamma = 10^{-8}$ fixed. These graphs show that T_2 possesses a minimum and two maxima. The crack tip is not stress-free. The maximum of T_2 occur close to the dislocation. For example, in the case $\bar{x}_0 = 3.1$, the maximum is at $\bar{x}_c \simeq 4.4$ and in the case $\bar{x}_0 = 10.1$ it is at $\bar{x}_c = 11.2$.

To obtain an idea on the combined effect I have selected $\beta = 10^{-4}$ and plotted the ratio of the combined stress to $\sigma_0(t_{\theta z}/\sigma_0)$ in Fig. 5 for various $\bar{x}_0$. From these graphs it is clear that when

the dislocation is located close to the maximum of T_1 the combined effect is large. For example, while $T_{1max} \simeq 0.451$ for the case of crack alone, for the combined effect we have $T_{max} = 0.63$ so that the ratio of the two K_g-values is given by

$$K_{gtot} / K_{g1} \simeq 0.71 \tag{6.6}$$

This implies that a dislocation located at a distance approximately one or two lattice parameters away from the crack tip reduces the fracture toughness by about 30%. Hence the theoretical values of K_g listed in Table 1 will be reduced about 30% bringing the numbers on the last column closer to those listed in the adjacent column marked experiments. These results however must still be considered only as indications for the trend. A more realistic physical picture requires the presence of large numbers of dislocations distributed over a few microns or so distance, away from the crack tip. Consequently, to obtain a close approximation to experimental observations of Chang and Ohr we need to consider a distribution of dislocation in a region near the crack tip. Such a consideration will require a separate study of dislocation pile up which is left to a future study.

Acknowledgment

Present work was supported by the Office of Naval Research. The author is indebted to Dr. N. Basdekas for his encouragement and enthusiasm I wish to thank Drs. S.M. Ohr and S.-J. Chang, for many valuable discussions and Mr. A. Suresh for the computer work.

REFERENCES

[1] J.P. Hirth and J. Lothe, "Theory of Dislocations", McGraw-Hill, New York, 1968, Ch. 8.

[2] A.A. Griffith, Phil. Trans. Roy. Soc., A221, 163, 1920.

[3] A.C. Eringen, C.G. Speziale and B.S. Kim, J. Mech. Phys. Solids, 25, 339 (1977).

[4] A.C. Eringen, Int. J. of Fracture, 14, 367 (1978)

[5] A.C. Eringen, Nonlinear Equations in Physics and Mathematics (Edited by A.O. Barut), Reidel Pub. Co., Holland, 271-318 (1978).

[6] A.C. Eringen, J. Phys. D. Appl. Phys., 10, 671 (1977).

[7] A.C. Eringen, and D.G.B. Edelen, Int. J. Engng. Sci., 10, 233 (1972).

[8] A.C. Eringen, Int. J. Engng. Sci., 10, 425 (1972).

[9] A.C. Eringen, Continuum Physics, Vol. IV, 204-267, Academic Press (1976).

[10] N. Ari, and A.C. Eringen, "Nonlocal Stress Field at Griffith Crack," Crystal Lattice Defects and Amorph. Mat. 10, 33, 1983.

[11] A.C. Eringen and B.S. Kim, Crystal Lattice Defects, 7, 51 (1977).

[12] N.P. Louat, Proc. Int. Conf. on Fracture, 117, Sendai, Japan (1965).

[13] F.G. Tricomi, Quart. J. Math. Oxford 2, 199, 1951.

[14] A. Kelly, Strong Solids, 12, Oxford 1966.

[15] S.M. Ohr, J.A. Horton and S.-J. Chang, "Direct Observations of Crack Tip Dislocation Behavior During Tensile and Cyclic Deformation," Technical Report, Oak Ridge National Laboratory.

[16] S.M. Ohr, and S.-J. Chang, J. Appl. Phys., 53, 5645, 1982.

[17] C. Kittel, Introduction to Solid State Physics, 4th ed. p.38, John Wiley, 1974.

[18] J. Rice and R. Thomson, Phil. Mag., 29, 73 (1974).

[19] A. Kelly, W.R. Tyson and A.H. Cottrell, Phil. Mag. 15, 567 (1967)

Table 1 : Critical Stress Intensity Factors

Material	$a(10^{-8}cm)$[17]	$\mu(10^{11}cgs)$[18]	$\gamma_s(cgs)$[18]	$t_y(10^{11}cgs)$[19]	Classical $K_c/t_y(10^{-3}cm^{\frac{1}{2}})$	Experiment[16] $K/t_y(10^{-3}cm^{\frac{1}{2}})$	Present $K_g/t_y(10^{-3}cm^{\frac{1}{2}})$
Al (fcc)	4.05	2.51	840	0.262	1.11	0.31	0.49
Cu (fcc)	3.61	4.05	1688	0.137	3.86	0.66	0.47
Ni (fcc)	3.52	7.48	1725	0.274	2.62	0.66	0.46
Fe (bcc)	2.87	6.9	1975	0.71	1.04	0.23	0.42

LIST OF FIGURES

Figure 1: Dispersion Curves for the Present Nonlocal Model and the Born-Kármán Model of Lattice Dynamics

Figure 2: Crack Subject to Anti-Plane Shear (Mode III)

Figure 3: Non-Dimensional Shear (No Dislocation)

Figure 4: Non-Dimensional Shear Stress Due to Dislocation Interaction

Figure 5: Total Shear Stress (Crack and Dislocation)

LIST OF TABLES

Table 1: Critical Stress Intensity Factors

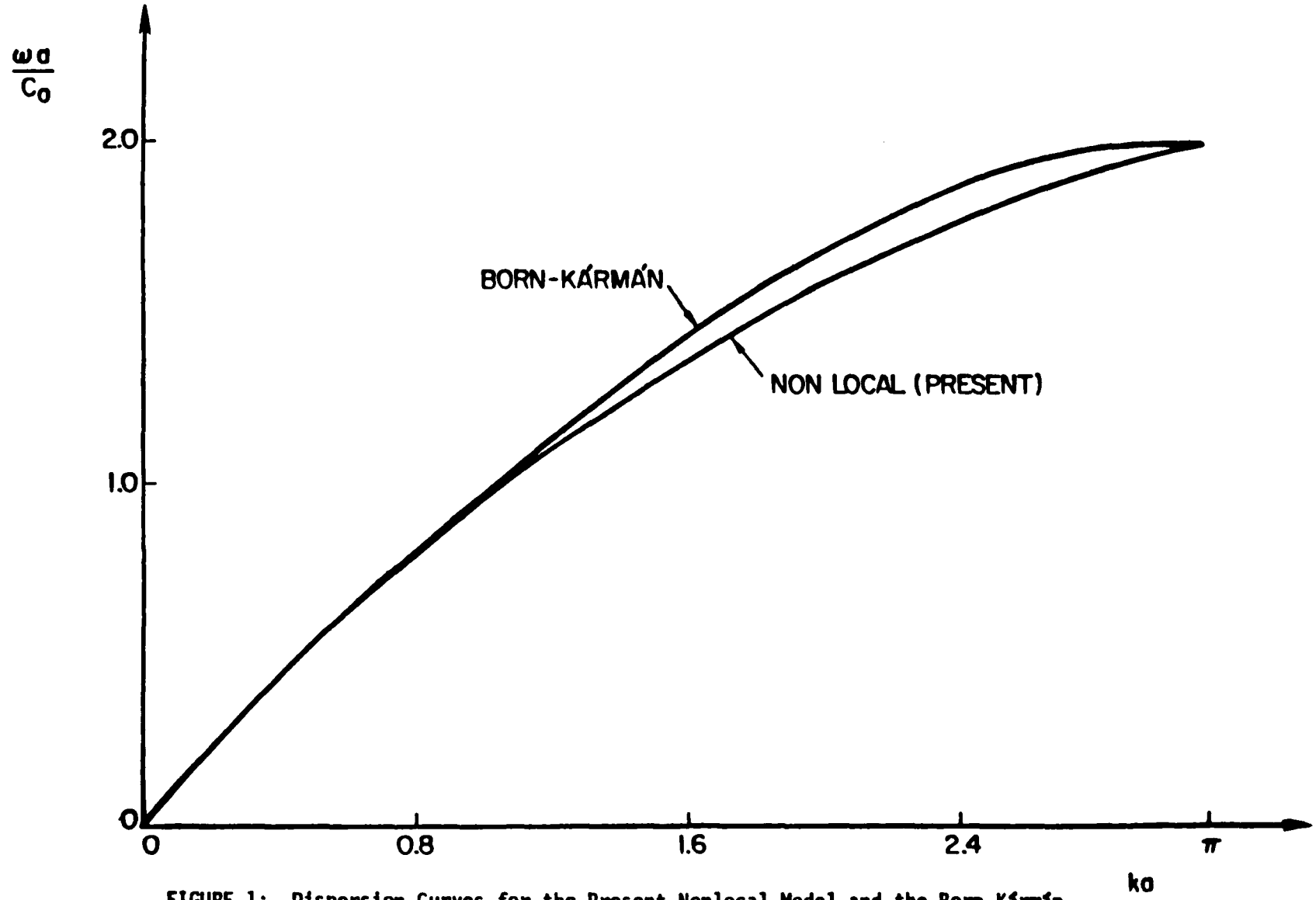

FIGURE 1: Dispersion Curves for the Present Nonlocal Model and the Born-Kármán Model of Lattice Dynamics

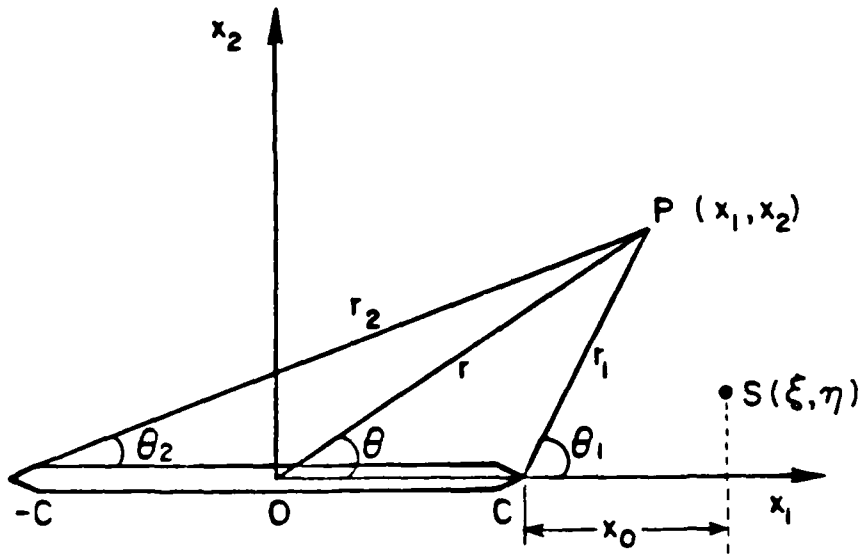

CRACK SUBJECT TO ANTI-PLANE SHEAR (MODE III)

FIGURE 2

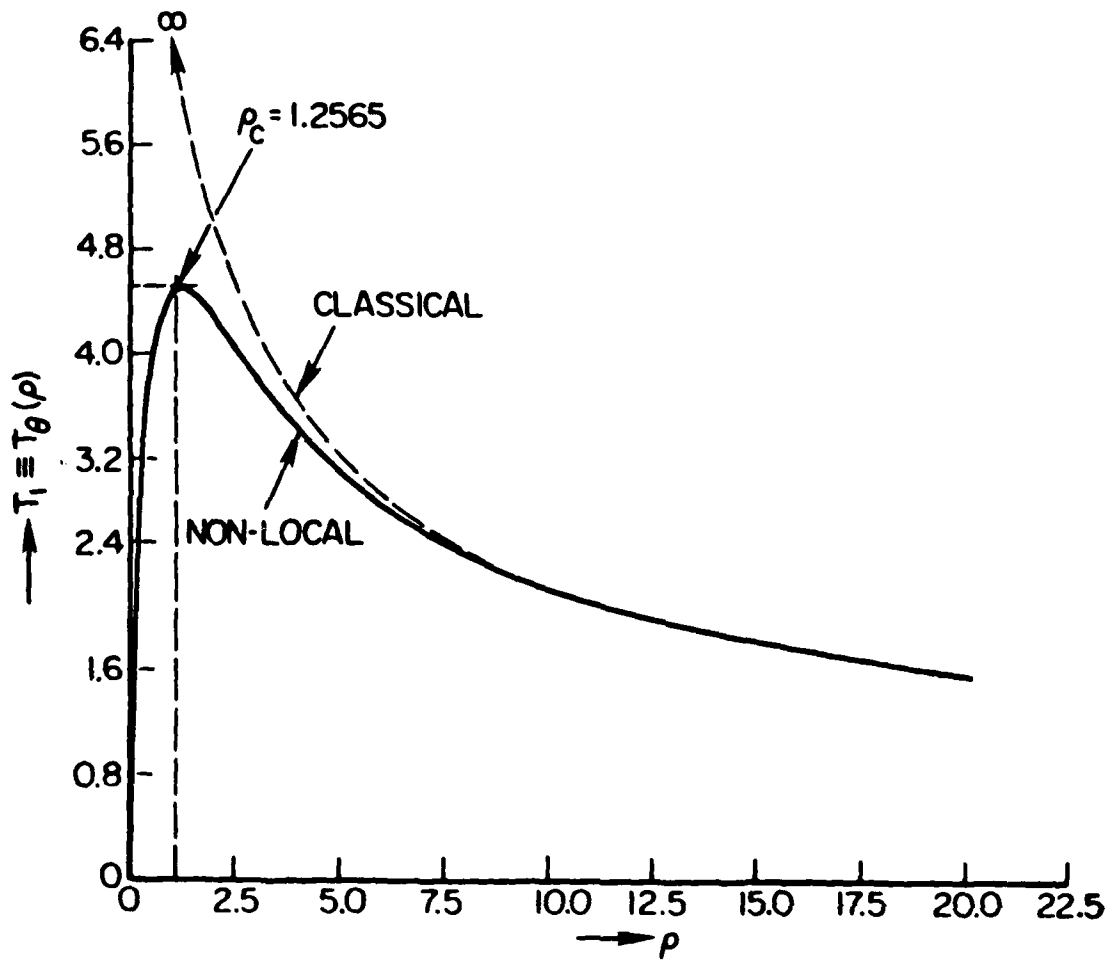

NON-DIMENSIONAL SHEAR (NO DISLOCATION)

FIGURE 3

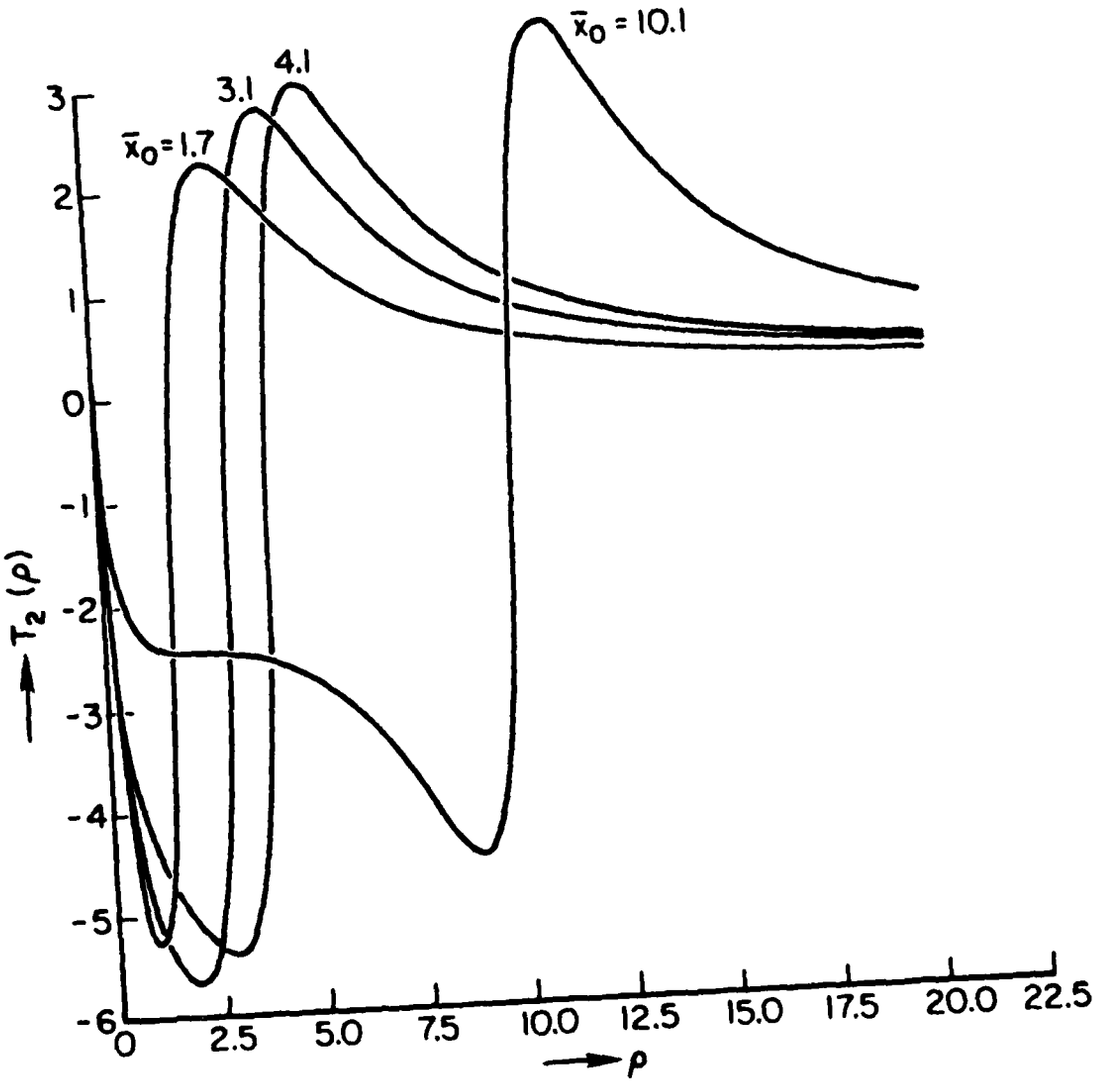

NON-DIMENSIONAL SHEAR STRESS DUE TO DISLOCATION INTERACTION

FIGURE 4

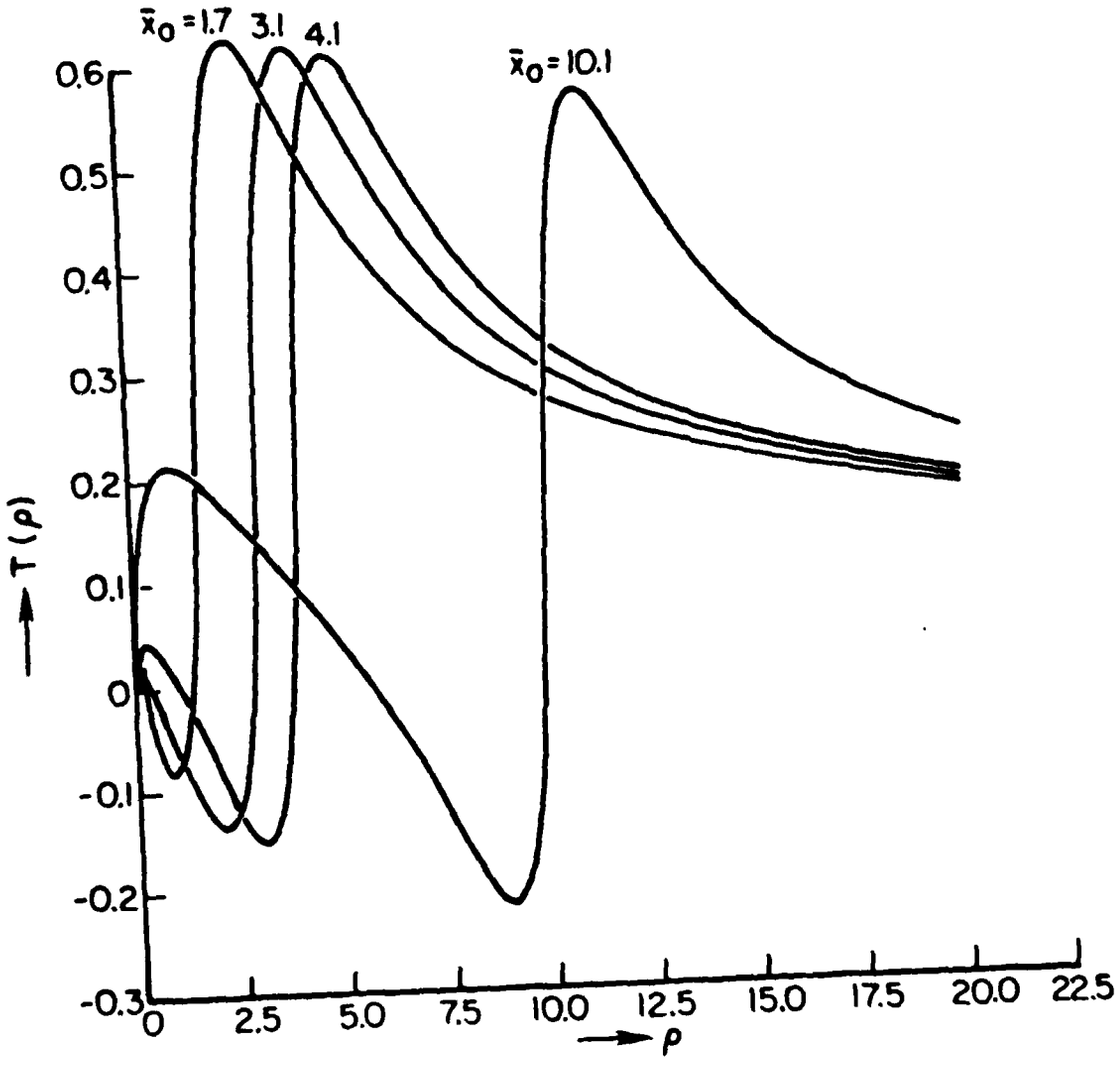

TOTAL SHEAR STRESS (CRACK AND DISLOCATION)

FIGURE 5

Part 1 - Government
Administrative and Liaison Activities

Office of Naval Research
Department of the Navy
Arlington, Virginia 22217
Attn: Code 474 (2)
Code 471
Code 200

Director
Office of Naval Research
Eastern/Central Regional Office
666 Summer Street
Boston, Massachusetts 02210

Director
Office of Naval Research
Branch Office
536 South Clark Street
Chicago, Illinois 60605

Director
Office of Naval Research
New York Area Office
715 Broadway - 5th Floor
New York, New York 10003

Director
Office of Naval Research
Western Regional Office
1030 East Green Street
Pasadena, California 91106

Naval Research Laboratory (6)
Code 2627
Washington, D.C. 20375

Defense Technical Information Center (12)
Cameron Station
Alexandria, Virginia 22314

Navy

Undersea Explosion Research Division
Naval Ship Research and Development
Center
Norfolk Naval Shipyard
Portsmouth, Virginia 23709
Attn: Dr. E. Palmer, Code 177

Navy (Con't.)

Naval Research Laboratory
Washington, D.C. 20375
Attn: Code 8400
8410
8430
8440
6300
6390
6380

David W. Taylor Naval Ship Research
and Development Center
Annapolis, Maryland 21402
Attn: Code 2740
28
281

Naval Weapons Center
China Lake, California 93555
Attn: Code 4062
4520

Commanding Officer
Naval Civil Engineering Laboratory
Code L31
Port Hueneme, California 93041

Naval Surface Weapons Center
White Oak
Silver Spring, Maryland 20910
Attn: Code R-10
G-402
K-82

Technical Director
Naval Ocean Systems Center
San Diego, California 92152

Supervisor of Shipbuilding
U.S. Navy
Newport News, Virginia 23607

Navy Underwater Sound
Reference Division
Naval Research Laboratory
P.O. Box 8337
Orlando, Florida 32806

Chief of Naval Operations
Department of the Navy
Washington, D.C. 20350
Attn: Code OP-098

Navy (Con't.)

Strategic Systems Project Office
Department of the Navy
Washington, D.C. 20376
Attn: NSP-200

Naval Air Systems Command
Department of the Navy
Washington, D.C. 20361
Attn: Code 5302 (Aerospace and Structures)
604 (Technical Library)
320B (Structures)

Naval Air Development Center
Warminster, Pennsylvania 18974
Attn: Aerospace Mechanics
Code 606

U.S. Naval Academy
Engineering Department
Annapolis, Maryland 21402

Naval Facilities Engineering Command
200 Stovall Street
Alexandria, Virginia 22332
Attn: Code 03 (Research and Development)
04B
045
14114 (Technical Library)

Naval Sea Systems Command
Department of the Navy
Washington, D.C. 20362
Attn: Code 05H
312
322
323
05R
32R

Navy (Con't.)

Commander and Director
David W. Taylor Naval Ship
Research and Development Center
Bethesda, Maryland 20084
Attn: Code 042
17
172
173
174
1800
1844
012.2
1900
1901
1945
1960
1962

Naval Underwater Systems Center
Newport, Rhode Island 02840
Attn: Bruce Sandman, Code 3634

Naval Surface Weapons Center
Dahlgren Laboratory
Dahlgren, Virginia 22448
Attn: Code G04
G20

Technical Director
Mare Island Naval Shipyard
Vallejo, California 94592

U.S. Naval Postgraduate School
Library
Code 0384
Monterey, California 93940

Webb Institute of Naval Architecture
Attn: Librarian
Crescent Beach Road, Glen Cove
Long Island, New York 11542

Army

Commanding Officer (2)
U.S. Army Research Office
P.O. Box 12211
Research Triangle Park, NC 27709
Attn: Mr. J. J. Murray, CRD-AA-IP

Army (Con't.)

Watervliet Arsenal
MAGGS Research Center
Watervliet, New York 12189
Attn: Director of Research

U.S. Army Materials and Mechanics
Research Center
Watertown, Massachusetts 02172
Attn: Dr. R. Shea, DRXMR-T

U.S. Army Missile Research and
Development Center
Redstone Scientific Information
Center
Chief, Document Section
Redstone Arsenal, Alabama 35809

Army Research and Development
Center
Fort Belvoir, Virginia 22060

NASA

National Aeronautics and Space
Administration
Structures Research Division
Langley Research Center
Langley Station
Hampton, Virginia 23365

National Aeronautics and Space
Administration
Associate Administrator for Advanced
Research and Technology
Washington, D.C. 20546

Air Force

Wright-Patterson Air Force Base
Dayton, Ohio 45433
Attn: AFFDL (FB)
(FBR)
(FBE)
(FBS)
AFML (MBM)

Chief Applied Mechanics Group
U.S. Air Force Institute of Technology
Wright-Patterson Air Force Base
Dayton, Ohio 45433

Air Force (Con't.)

Chief, Civil Engineering Branch
WLRC, Research Division
Air Force Weapons Laboratory
Kirtland Air Force Base
Albuquerque, New Mexico 87117

Air Force Office of Scientific Research
Bolling Air Force Base
Washington, D.C. 20332
Attn: Mechanics Division

Department of the Air Force
Air University Library
Maxwell Air Force Base
Montgomery, Alabama 36112

Other Government Activities

Commandant
Chief, Testing and Development Division
U.S. Coast Guard
1300 E Street, NW.
Washington, D.C. 20226

Technical Director
Marine Corps Development
and Education Command
Quantico, Virginia 22134

Director Defense Research
and Engineering
Technical Library
Room 3C128
The Pentagon
Washington, D.C. 20301

Dr. M. Gaus
National Science Foundation
Environmental Research Division
Washington, D.C. 20550

Library of Congress
Science and Technology Division
Washington, D.C. 20540

Director
Defense Nuclear Agency
Washington, D.C. 20305
Attn: SPSS

Other Government Activities (Con't)

Mr. Jerome Persh
Staff Specialist for Materials
and Structures
OUSDR&E, The Pentagon
Room 3D1089
Washington, D.C. 20301

Chief, Airframe and Equipment Branch
FS-120
Office of Flight Standards
Federal Aviation Agency
Washington, D.C. 20553

National Academy of Sciences
National Research Council
Ship Hull Research Committee
2101 Constitution Avenue
Washington, D.C. 20418
Attn: Mr. A. R. Lytle

National Science Foundation
Engineering Mechanics Section
Division of Engineering
Washington, D.C. 20550

Picatinny Arsenal
Plastics Technical Evaluation Center
Attn: Technical Information Section
Dover, New Jersey 07801

Maritime Administration
Office of Maritime Technology
14th and Constitution Avenue, NW.
Washington, D.C. 20230

PART 2 - Contractors and Other Technical Collaborators

Universities

Dr. J. Tinsley Oden
University of Texas at Austin
345 Engineering Science Building
Austin, Texas 78712

Professor Julius Miklowitz
California Institute of Technology
Division of Engineering
and Applied Sciences
Pasadena, California 91109

Universities (Con't)

Dr. Harold Liebowitz, Dean
School of Engineering and
Applied Science
George Washington University
Washington, D.C. 20052

Professor Eli Sternberg
California Institute of Technology
Division of Engineering and
Applied Sciences
Pasadena, California 91109

Professor Paul M. Naghdi
University of California
Department of Mechanical Engineering
Berkeley, California 94720

Professor A. J. Durelli
Oakland University
School of Engineering
Rochester, Missouri 48063

Professor F. L. DiMaggio
Columbia University
Department of Civil Engineering
New York, New York 10027

Professor Norman Jones
The University of Liverpool
Department of Mechanical Engineering
P. O. Box 147
Brownlow Hill
Liverpool L69 3BX
England

Professor E. J. Skudrzyk
Pennsylvania State University
Applied Research Laboratory
Department of Physics
State College, Pennsylvania 16801

Professor J. Klosner
Polytechnic Institute of New York
Department of Mechanical and
Aerospace Engineering
333 Jay Street
Brooklyn, New York 11201

Professor R. A. Schapery
Texas A&M University
Department of Civil Engineering
College Station, Texas 77843

Universities (Con't.)

Professor Walter D. Pilkey
University of Virginia
Research Laboratories for the
Engineering Sciences and
Applied Sciences
Charlottesville, Virginia 22901

Professor K. D. Willmert
Clarkson College of Technology
Department of Mechanical Engineering
Potsdam, New York 13676

Dr. Walter E. Haisler
Texas A&M University
Aerospace Engineering Department
College Station, Texas 77843

Dr. Hussein A. Kamel
University of Arizona
Department of Aerospace and
Mechanical Engineering
Tucson, Arizona 85721

Dr. S. J. Fenves
Carnegie-Mellon University
Department of Civil Engineering
Schenley Park
Pittsburgh, Pennsylvania 15213

Dr. Ronald L. Huston
Department of Engineering Analysis
University of Cincinnati
Cincinnati, Ohio 45221

Professor G. C. M. Sih
Lehigh University
Institute of Fracture and
Solid Mechanics
Bethlehem, Pennsylvania 18015

Professor Albert S. Kobayashi
University of Washington
Department of Mechanical Engineering
Seattle, Washington 98105

Professor Daniel Frederick
Virginia Polytechnic Institute and
State University
Department of Engineering Mechanics
Blacksburg, Virginia 24061

Universities (Con't)

Professor A. C. Eringen
Princeton University
Department of Aerospace and
Mechanical Sciences
Princeton, New Jersey 08540

Professor E. H. Lee
Stanford University
Division of Engineering Mechanics
Stanford, California 94305

Professor Albert I. King
Wayne State University
Biomechanics Research Center
Detroit, Michigan 48202

Dr. V. R. Hodgson
Wayne State University
School of Medicine
Detroit, Michigan 48202

Dean B. A. Boley
Northwestern University
Department of Civil Engineering
Evanston, Illinois 60201

Professor P. G. Hodge, Jr.
University of Minnesota
Department of Aerospace Engineering
and Mechanics
Minneapolis, Minnesota 55455

Dr. D. C. Drucker
University of Illinois
Dean of Engineering
Urbana, Illinois 61801

Professor N. M. Newmark
University of Illinois
Department of Civil Engineering
Urbana, Illinois 61803

Professor E. Reissner
University of California, San Diego
Department of Applied Mechanics
La Jolla, California 92037

Professor William A. Nash
University of Massachusetts
Department of Mechanics and
Aerospace Engineering
Amherst, Massachusetts 01002

Universities (Con't)

Professor G. Herrmann
Stanford University
Department of Applied Mechanics
Stanford, California 94305

Professor J. D. Achenbach
Northwest University
Department of Civil Engineering
Evanston, Illinois 60201

Professor S. B. Dong
University of California
Department of Mechanics
Los Angeles, California 90024

Professor Burt Paul
University of Pennsylvania
Towne School of Civil and
Mechanical Engineering
Philadelphia, Pennsylvania 19104

Professor H. W. Liu
Syracuse University
Department of Chemical Engineering
and Metallurgy
Syracuse, New York 13210

Professor S. Bodner
Technion R&D Foundation
Haifa, Israel

Professor Werner Goldsmith
University of California
Department of Mechanical Engineering
Berkeley, California 94720

Professor R. S. Rivlin
Lehigh University
Center for the Application
of Mathematics
Bethlehem, Pennsylvania 18015

Professor F. A. Cozzarelli
State University of New York at
Buffalo
Division of Interdisciplinary Studies
Karr Parker Engineering Building
Chemistry Road
Buffalo, New York 14214

Universities (Con't)

Professor Joseph L. Rose
Drexel University
Department of Mechanical Engineering
and Mechanics
Philadelphia, Pennsylvania 19104

Professor B. K. Donaldson
University of Maryland
Aerospace Engineering Department
College Park, Maryland 20742

Professor Joseph A. Clark
Catholic University of America
Department of Mechanical Engineering
Washington, D.C. 20064

Dr. Samuel B. Batdorf
University of California
School of Engineering
and Applied Science
Los Angeles, California 90024

Professor Isaac Fried
Boston University
Department of Mathematics
Boston, Massachusetts 02215

Professor E. Krempl
Rensselaer Polytechnic Institute
Division of Engineering
Engineering Mechanics
Troy, New York 12181

Dr. Jack R. Vinson
University of Delaware
Department of Mechanical and Aerospace
Engineering and the Center for
Composite Materials
Newark, Delaware 19711

Dr. J. Duffy
Brown University
Division of Engineering
Providence, Rhode Island 02912

Dr. J. L. Swedlow
Carnegie-Mellon University
Department of Mechanical Engineering
Pittsburgh, Pennsylvania 15213

Universities (Con't)

Dr. V. K. Varadan
Ohio State University Research Foundation
Department of Engineering Mechanics
Columbus, Ohio 43210

Dr. Z. Hashin
University of Pennsylvania
Department of Metallurgy and
Materials Science
College of Engineering and
Applied Science
Philadelphia, Pennsylvania 19104

Dr. Jackson C. S. Yang
University of Maryland
Department of Mechanical Engineering
College Park, Maryland 20742

Professor T. Y. Chang
University of Akron
Department of Civil Engineering
Akron, Ohio 44325

Professor Charles W. Bert
University of Oklahoma
School of Aerospace, Mechanical,
and Nuclear Engineering
Norman, Oklahoma 73019

Professor Satya N. Atluri
Georgia Institute of Technology
School of Engineering and
Mechanics
Atlanta, Georgia 30332

Professor Graham F. Carey
University of Texas at Austin
Department of Aerospace Engineering
and Engineering Mechanics
Austin, Texas 78712

Dr. S. S. Wang
University of Illinois
Department of Theoretical and
Applied Mechanics
Urbana, Illinois 61801

Professor J. F. Abel
Cornell University
Department of Theoretical
and Applied Mechanics
Ithaca, New York 14853

Universities (Con't)

Professor V. H. Neubert
Pennsylvania State University
Department of Engineering Science
and Mechanics
University Park, Pennsylvania 16802

Professor A. W. Leissa
Ohio State University
Department of Engineering Mechanics
Columbus, Ohio 43212

Professor C. A. Brebbia
University of California, Irvine
Department of Civil Engineering
School of Engineering
Irvine, California 92717

Dr. George T. Hahn
Vanderbilt University
Mechanical Engineering and
Materials Science
Nashville, Tennessee 37235

Dean Richard H. Gallagher
University of Arizona
College of Engineering
Tucson, Arizona 85721

Professor E. F. Rybicki
The University of Tulsa
Department of Mechanical Engineering
Tulsa, Oklahoma 74104

Dr. R. Haftka
Illinois Institute of Technology
Department of Mechanics and Mechanical
and Aerospace Engineering
Chicago, Illinois 60616

Professor J. G. de Oliveira
Massachusetts Institute of Technology
Department of Ocean Engineering
77 Massachusetts Avenue
Cambridge, Massachusetts 02139

Dr. Bernard W. Shaffer
Polytechnic Institute of New York
Route 110
Farmingdale, New York 11735

474:NP:716:lab
78u474-619

Industry and Research Institutes

Dr. Norman Hobbs
Kaman AviDyne
Division of Kaman
Sciences Corporation
Burlington, Massachusetts 01803

Argonne National Laboratory
Library Services Department
9700 South Cass Avenue
Argonne, Illinois 60440

Dr. M. C. Junger
Cambridge Acoustical Associates
54 Rindge Avenue Extension
Cambridge, Massachusetts 02140

Mr. J. H. Torrance
General Dynamics Corporation
Electric Boat Division
Groton, Connecticut 06340

Dr. J. E. Greenspon
J. G. Engineering Research Associates
3831 Menlo Drive
Baltimore, Maryland 21215

Newport News Shipbuilding and
Dry Dock Company
Library
Newport News, Virginia 23607

Dr. W. F. Bozich
McDonnell Douglas Corporation
5301 Bolsa Avenue
Huntington Beach, California 92647

Dr. H. N. Abramson
Southwest Research Institute
8500 Culebra Road
San Antonio, Texas 78284

Dr. R. C. DeHart
Southwest Research Institute
8500 Culebra Road
San Antonio, Texas 78284

Dr. M. L. Baron
Weidlinger Associates
110 East 59th Street
New York, New York 10022

Industry and Research Institutes (Con't)

Dr. T. L. Geers
Lockheed Missiles and Space Company
3251 Hanover Street
Palo Alto, California 94304

Mr. William Caywood
Applied Physics Laboratory
Johns Hopkins Road
Laurel, Maryland 20810

Dr. Robert E. Dunham
Pacifica Technology
P.O. Box 148
Del Mar, California 92014

Dr. M. F. Kanninen
Battelle Columbus Laboratories
505 King Avenue
Columbus, Ohio 43201

Dr. A. A. Hochrein
Daedalean Associates, Inc.
Springlake Research Road
15110 Frederick Road
Woodbine, Maryland 21797

Dr. James W. Jones
Swanson Service Corporation
P.O. Box 5415
Huntington Beach, California 92646

Dr. Robert E. Nickell
Applied Science and Technology
3344 North Torrey Pines Court
Suite 220
La Jolla, California 92037

Dr. Kevin Thomas
Westinghouse Electric Corp.
Advanced Reactors Division
P. C. Box 158
Madison, Pennsylvania 15663

Dr. H. D. Hibbitt
Hibbitt & Karlsson, Inc.
132 George M. Cohan Boulevard
Providence, Rhode Island 02903

Dr. R. D. Mindlin
89 Deer Hill Drive
Ridgefield, Connecticut 06877

474:NP:716:lab
78u474-619

Industry and Research Institutes (Con't)

Dr. Richard E. Dame
Mega Engineering
11961 Tech Road
Silver Spring, Maryland 20904

Mr. G. M. Stanley
Lockheed Palo Alto Research
Laboratory
3251 Hanover Street
Palo Alto, California 94304

Mr. R. L. Cloud
Robert L. Cloud Associates, Inc.
2972 Adeline Street
Berkeley, California 94703

MED

8